Accepted Manuscript

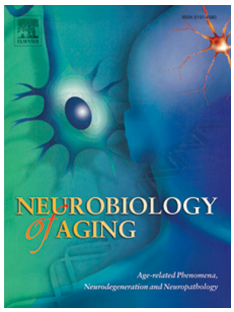

APP/Go protein Gβγ complex signaling mediates Aβ degeneration and cognitive impairment in Alzheimer´s disease models

Elena Anahi Bignante, Nicolás Eric Ponce, Florencia Heredia, Juliana Musso, María C. Krawczyk, Julieta Millán, Gustavo F. Pigino, Nibaldo C. Inestrosa, Mariano M. Boccia, Alfredo Lorenzo

PII: S0197-4580(17)30408-6

DOI: 10.1016/j.neurobiolaging.2017.12.013

Reference: NBA 10109

To appear in: *Neurobiology of Aging*

Received Date: 16 August 2017

Revised Date: 5 December 2017

Accepted Date: 10 December 2017

Please cite this article as: Bignante, E.A., Ponce, N.E., Heredia, F., Musso, J., Krawczyk, M.C., Millán, J., Pigino, G.F., Inestrosa, N.C., Boccia, M.M., Lorenzo, A., APP/Go protein Gβγ complex signaling mediates Aβ degeneration and cognitive impairment in Alzheimer´s disease models, *Neurobiology of Aging* (2018), doi: 10.1016/j.neurobiolaging.2017.12.013.

APP/Go protein Gβγ complex signaling mediates Aβ degeneration and cognitive impairment in Alzheimer´s disease models

Elena Anahi Bignante[1,6], Nicolás Eric Ponce[1]; Florencia Heredia[1], Juliana Musso[1], María C. Krawczyk[2], Julieta Millán [2], Gustavo F. Pigino[1], Nibaldo C. Inestrosa[3,4], Mariano M. Boccia[2] and Alfredo Lorenzo[1,5]

[1]Instituto de Investigación Médica "Mercedes y Martín Ferreyra", INIMEC-CONICET- Universidad Nacional de Córdoba, Casilla de Correo 389, 5000, Córdoba, ARGENTINA. [2]Laboratorio de Neurofarmacología de los Procesos de Memoria, Cátedra de Farmacología, Facultad de Farmacia y Bioquímica, Universidad de Buenos Aires, Junín 956, 5to piso, Buenos Aires, Argentina.[3]Centro de Envejecimiento y Regeneración (CARE), Facultad de Ciencias Biológicas, Pontificia Universidad Católica de Chile, Alameda 340, P. O.Box 114-D, Santiago, Chile. [4]Centro de Excelencia en Biomedicina de Magallanes (CEBIMA), Punta Arenas, Chile. [5]Departamento de Farmacología, Facultad de Ciencias Químicas, Universidad Nacional de Córdoba, ARGENTINA. [6]Instituto Universitario de Ciencias Biomédicas de Córdoda (IUCBC), ARGENTINA.

Corresponding author:

Alfredo Lorenzo

alorenzo@immf.uncor.edu

Instituto de Investigación Médica "Mercedes y Martín Ferreyra", INIMEC-CONICET- Universidad Nacional de Córdoba, Casilla de Correo 389, 5000, Córdoba, ARGENTINA

Abstract

Deposition of Amyloid-β (Aβ), the proteolytic product of the Amyloid Precursor protein (APP), might cause neurodegeneration and cognitive decline in Alzheimer's disease (AD). However, the direct involvement of APP in the mechanism of Aβ-induced degeneration in AD remains on debate. Here, we analyzed the interaction of APP with heterotrimeric Go protein in primary hippocampal cultures and found that Aβ deposition dramatically enhanced APP-Go protein interaction in dystrophic neurites. APP-overexpression rendered neurons vulnerable to Aβ-toxicity by a mechanism that required Go-Gβγ complex signaling and p38-MAPK activation. Gallein, a selective pharmacological inhibitor of Gβγ complex, inhibited Aβ-induced dendritic and axonal dystrophy, abnormal tau phosphorylation, synaptic loss and neuronal cell death in hippocampal neurons expressing endogenous protein levels. In the 3xTg-AD mice, intrahippocampal application of gallein reversed memory impairment associated with early Aβ-patology. Our data provide further evidence for the involvement of APP/Go protein in Aβ-induced degeneration, and reveal that Gβγ complex is a signaling target potentially relevant for developing therapies for halting Aβ-degeneration in AD.

Keywords

Alzheimer, Amyloid β (Aβ), Amyloid Precursor protein (APP), Go protein, Gβγ complex, degeneration, 3xTg-AD mice.

Highlights

- Aβ deposition enhances APP/Go protein interaction in dystrophic neurites.
- APP mediates Aβ-toxicity through Go protein Gβγ signaling and p38-MAPK activation.
- Inhibition of Gβγ signaling abrogates Aβ-toxicity in *in vitro* and *in vivo* AD models.
- APP/Go Gβγ complex might be a therapeutic target for halting degeneration in AD.

Abbreviations

AD: Alzheimer's disease; APP: Amyloid Precursor protein; Aβ: Amyloid-β peptide; MAP2: microtubule associate protein 2; FRET: fluorescence resonance energy transfer; GPCR: G protein-coupled receptor; βARK: β adrenergic receptor kinase; NOR: novel object recognition.

Introduction

Alzheimer's disease (AD) is the most frequent neurodegenerative pathology in the elderly human population with no effective therapy. AD is characterized by progressive decline of cognitive functions leading to dementia in advanced stages. Pathologic hallmarks of AD include Amyloid β (Aβ) plaques, neurofibrillary tangles mainly composed of abnormally phosphorylated tau, dystrophic neurites surrounding Aβ plaques and overt loss of synapses and neurons (Nelson et al., 2012). The dominant hypothesis posits that deposition of toxic Aβ aggregates leads to progressive neurodegeneration, altering circuits for cognitive functions (Selkoe and Hardy, 2016). Accordingly, rational therapies for AD should aim to clear Aβ aggregates or to inhibit signaling cascade triggered by neurotoxic Aβ assemblies.

Aβ is a 40-42 amino acid peptide derived from a regulated enzymatic processing of Amyloid Precursor protein (APP). In brain tissue, APP processing and Aβ production correlate with neuronal activity (Cirrito et al., 2005; Selkoe and Hardy, 2016). In pathological conditions Aβ aggregates and becomes toxic. The mechanism of Aβ neurotoxicity remains controversial likely because different Aβ assemblies induce neurodegeneration through distinct mechanisms (Dahlgren et al., 2002; Deshpande et al., 2006). Many signaling cascades and receptor-candidates for toxic Aβ aggregates have been proposed, among them APP emerges due to its strong linkage to AD (Bignante et al., 2013). Therefore, asserting the molecular mechanisms by which APP causes pathology is instrumental for developing rational therapies for AD.

Heterotrimeric guanine nucleotide-binding proteins (G proteins) are evolutionary conserved, widely used signal transduction systems composed of an alpha subunit (Gα) and a beta-gamma complex (Gβγ). G proteins are activated by G protein-coupled receptors (GPCR), which typically are seven transmembrane domain proteins though unconventional single membrane pass proteins have also been characterized (Patel, 2004). Ligand-binding to GPCR causes exchange of GTP for GDP bound to Gα, Gα-GTP and Gβγ complex dissociate and both can independently activate downstream signaling cascades (Marinissen and Gutkind, 2001). Increasing evidence support the role of APP as a GPCR that mainly interacts with heterotrimeric Go protein (Nishimoto et al., 1993) with an evolutionary conserved function (Copenhaver and Kogel, 2017). Several ligands for APP were identified, including physiologic APP-fragments sAPP and Aβ, which stimulate neuronal survival and synaptic activity by Go activation (Fogel et al., 2014; Milosch et al., 2014). Significantly, APP also binds toxic Aβ aggregates (Lorenzo et al., 2000; Van Nostrand et al., 2002) suggesting its contribution to neurodegeneration. In fact, APP-knockout neurons are less sensitive to Aβ-toxicity (Lorenzo et al., 2000) while overexpression of wild-type APP renders neurons vulnerable to Aβ-toxicity by Go signaling activation (Sola Vigo et al., 2009). Moreover, overexpression of APP carrying familial Alzheimer´s disease (FAD) mutations (FAD-APP) per se causes neuronal cell death also by Go activation (McPhie et al., 2003; Niikura et al., 2004). Importantly, recent observations on new FAD-APP knock-in mice revealed that many mechanisms of neurodegeneration previously described might be artifacts caused by APP overexpression (Saito et al., 2016). Hence, it remains to be determined whether APP-Go signaling effectively contributes to Aβ-induced toxicity in neurons expressing endogenous protein levels.

In the present work, we used APP-transfected and non-transfected hippocampal neurons and the 3xTg-AD mice model of AD to assess the role of APP/Go protein signaling in Aβ-induced degeneration and cognitive dysfunction. We uncovered that APP/Go protein Gβγ complex

constitutes a signaling hub with potential therapeutic value for halting Aβ degeneration and cognitive impairment in AD.

Materials and Methods

Animals

Behavioral experiments were conducted in wild-type (control) and triple transgenic 3xTg-AD mice which have been previously characterized (Oddo et al., 2003). Briefly, the mice harbor APP (KM670/671NL) and Tau (P301L) mutations into a PS1M146V knock-in background. Non-Tg mice (control) were from the same strain and genetic background as the PS1-KI mice, but they harbor the endogenous wild-type mouse PS1 gene. Animals were originally donated by Dr. Frank LaFerla, UC Irvine, CA and bred in-house at the School of Pharmacy and Biochemistry, University of Buenos Aires from homozygous pairing. They were individually identified and housed 6-12 per cage in plastic cages (45 cm x 30 cm x 10 cm) with dry food and tap water *ad libitum* except during training and testing procedures. The mice were kept in acclimatized animal room (21–23℃) and maintained on a 12 h light/12 h dark cycle (lights on at 6:00 am). Behavioral experiments were carried out in female and male animals of 4.5-5 month of age, and experimental groups were balanced by sex. Statistical comparisons confirmed no significant difference between sexes in each experimental condition, therefore data from males and females were pooled. All animal procedures were performed in strict accordance with the guidelines of the Institutional Council of Animal Care CICUAL-INIMEC-CONICET and CICUAL-FFyB which follows the guidelines of the U.S: National Institute of Health Guide for the Care and Use of Laboratory Animals, and efforts were made to minimize the number of animals used and manipulations.

Cell cultures

Rat hippocampal cultures were established from embryonic day 18 fetuses (Wistar) as described previously (Heredia et al., 2004). Briefly, neurons were plated in DMEM (GIBCO) plus 10% horse serum (GBO) on poly-L-lysine (0.25 mg/ml, Sigma-Aldrich)-coated dishes. After 2h, medium was replaced with Neurobasal (GIBCO) plus B27 supplement (GIBCO). HEK293 cells were seeded and maintained in DMEM (GIBCO) supplemented with 10 % fetal bovine serum (FBS, GBO). Cell cultures were maintained at 37℃ in a 5% CO_2 humidified atmosphere.

Expression plasmids and transfections

Plasmids: Transfection were performed with plasmid pEYFP-N3 encoding the yellow fluorescent protein (YFP, Clontech) or plasmid pcDNA3.1 (Life Technology) encoding full-length wild-type human APP695 (APP), YFP fused to C-terminal domain of APP (APP-YFP), wild-type Goα subunit of Go protein, pertussis toxin-insensitive form of Goα protein (iPTX-Go) or β adrenergic receptor kinase C-terminal peptide (βARK). As controls the empty vector pcDNA3.1 (ev) was used. G protein-related plasmids were generously provided by Dr J. Silvio Gutkind (National Institutes of Health, Bethesda, MD, EEUU).

Transfections procedures: HEK293 cells (80 % confluence) were transfected with a mixture of 1.6 µg DNA and 0.05 mM Polyethyleneimine 87K (PEI, produced by Dr. Juan M Lázaro-Martinez, Universidad Nacional de Buenos Aires, Argentina) dissolved in NaCl 0.15 mM.

2-3 DIV hippocampal cultures were transfected as previously reported (Sola Vigo et al., 2009). Briefly, rat hippocampal cultures (700.000 cells/ cm2) grown in 96 multiwell plates were transfected with 40 ng/well of YFP-plasmid and 60 ng/well of pcDNA3.1 plasmid encoding the indicated protein by using Lipofectamine 2000 (0.4 µl/well; Life Technology) in 60µl/well DMEM (Life Technology). After 1 h, the transfection-medium was replaced with DMEM plus B27 supplement (Life Technology).

7 DIV rat hippocampal cultures (70.000 cells/cm2) grown in 12 mm coverslips were transfected with 8 µg APP-YFP plasmid and 4 µl Lipofectamine 2000 (Life Technology) in 1 ml Neurobasal medium (Life Technology). After 1 h the transfection-medium was washed and neurons were returned to its own conditioned culture media.

Reagents and treatments

Synthetic Aβ1-42, Aβ1-40 and Aβ 25-35 were obtained from Biopeptide Inc (San Diego, CA). Toxic Aβ was prepared as previously described (Heredia et al., 2004; Sola Vigo et al., 2009), and all experiments were replicated with all three Aβ peptides at 20 µM. Pertussis toxin (200-400 ng/ml; Sigma-Aldrich), p21-Activated Kinase inhibitor III (IPA-3, CAS 42521-82-4, 5µM, Calbiochem), c-Jun N-terminal kinase inhibitor II (SP600125, CAS 129-56-6; 1µM Calbiochem), extracellular-regulated kinase (ERK) inhibitor (PD 98059, CAS 167869-21-8; 50µM, Calbiochem), p38-MAPK inhibitor (SB 203580, CAS 152121-47-6, 20µM, Calbiochem), gallein (10µM, Santa Cruz) Pharmacological inhibitors were dissolved in DMSO and applied to cultured cells 30 min before Aβ-treatment.

The following antibodies were used: mouse anti-APP N-terminal clone 22C11 (1:500; Millipore), antibody B9 is a rabbit polyclonal antibody to Aβ-domain of APP (generously provided by Dr Bruce A. Yankner, Harvard University); rabbit anti-APP C-terminal clone Y188 (1:250, Abcam), mouse anti-Gαo clone A2 (1:500, Santa Cruz), rabbit polyclonal anti-Gαo K20 (1:500, Santa Cruz), mouse anti- neuron-specific class III β tubulin clone #TuJ1 (1:2000; Neuronomics), anti-phospho-p38 MAPK Thr180/Tyr182 (1:1000; Cell Signaling), anti-p38 MAPK (Cell Signaling), mouse anti-MAP2 clone AP-20 (1:500, Millipore), mouse anti-PSD95 clone 6G6-1C9 (1:250, Abcam), rabbit anti-synapthophysine H-93 (1:500, Santa Cruz), mouse monoclonal antibody to tau phosphorylated at Ser-396 and Ser-404 PHF-1 (1:1000) (Greenberg et al., 1992). For

immunofluorescence analysis primary antibodies were labeled with Alexa-conjugated secondary antibodies (488 or 568, Life Technology) and for western blot were labeled with Horseradish peroxidase-conjugated secondary antibody (Jackson ImmunoResearch) and visualized by ECL.

Immunolabeling, confocal microscopy and FRET

Methods for neuronal culture fixation and immunolabeling were described elsewhere (Heredia et al., 2006; Sola Vigo et al., 2009). Briefly, Cell cultures were fixed in 4% paraformaldehyde/0.12M sucrose in PBS for 30 min at 37oC, permeabilized for 5-7 minutes with 0.2% Triton X-100 in PBS and blocked for 30 min in 5% BSA or goat normal serum. The cells were then incubated overnight at 4oC with primary antibody followed by incubation in Alexa-conjugated secondary antibodies (Molecular Probes). Aβ fibrils were biotinylated (0,5 mg/ml, Sulpho-biotin, Pierce) and incubated with neutravidin Alexa 350 (Molecular Probes).

For colocalization analysis, confocal images were captured on an Olympus FV1000 Spectral microscope equipped with a PLAPON 60X Oil objective (1.42 NA) and Mander`s coefficient was calculated with FIJI software by using plugin Coloc2. For fluorescence resonance energy transfer (FRET) analysis, fluorescently labeled proteins were analyzed on an Olympus IX-71 inverted microscope equipped with a 60x plan apochromatic objective (NA = 1.4), a standard 488-568 FRET filter set, and an ANDOR iXon3 camera (DU-888E-C00-#BV). Repeated scans were applied during a 3 min period to achieve complete photobleaching of the Alexa568 acceptor protein. FRET efficiency (EM) was estimated as an increase of Alexa488 intensity (captured using a 505 nm filter cube) after the photobleaching of Alexa568. Acquired images were equally processed using Fiji software to generate FRET maps.

Immunoprecipitation and Western blot

Western blot: Cultures were harvested at 4ºC in RIPA buffer supplemented with protease inhibitors (SIGMAFAST, Sigma). The samples were diluted in Laemmli sample buffer, incubated at 95ºC for 5 min, resolved by PAGE, electrotransferred and incubated with the indicated primary antibodies followed by HRP-conjugated secondary antibody and visualized by ECL. For phospho-p38MAPK determination the band intensity was quantified by densitometric scanning using NIH Image J software (imagej.nih.gov/ij/) and the band intensity was normalized with respect to the corresponding total p38MAPK. Each treatment was performed in triplicate in three independent experiments.

Immunoprecipitation: Transfected HEK293 cells were lysed in non-denaturing buffer (25 mM HEPES pH:7,4, 5mM $MgCl_2$, 1% NP-40, 125 mM CH_3CO_2K, 10 % glycerol, supplemented with SIGMAFAST™ Protease Inhibitor Tablets; Sigma-Aldrich). Lysates were centrifuged at 14000 r.p.m. for 20 min and supernatants were collected (input). 350 µl of input sample were incubated over-night at 4ºC with primary antibodies followed by protein G Sepharose beads (Immunoprecipitation Starter Pack GE Healthcare Life Science). Prior to use protein G Sepharose beads were blocked with 5 % of albumin. Bead-bound antibody complexes were pelleted by centrifugation (2500 rpm 10 min), washed in lysis buffer and analyzed by western blot

Assessment of neuronal viability.

Methods for assessing neuronal viability in transfected cultures have been previously described (Kedikian et al., 2010; Sola Vigo et al., 2009). Briefly, YFP-fluorescence was used as a reporter of transfection and for neuronal viability. Therefore hippocampal cultures (1-3 DIV) were co-transfected with plasmid encoding for YFP together with plasmid encoding the indicated cDNA. Thereafter, identically transfected cultures were treated with vehicle (control) or Aβ for 6-8hs. Afterwards, images were taken at random in a fluorescence Zeiss microscopy with a 20 x objective in each experimental condition. Neurons exhibiting integrity of soma and at least two neurites three-times longer than the soma were scored as viable. Viability in each experimental

condition was calculated as a ratio of cell numbers in identically transfected cultures that were treated with vehicle vs Aβ. At least 200 neurons were scored in control condition.

Methods for assessing neuronal viability in non-transfected mature 10-14 DIV hippocampal cultures have been previously described (Heredia et al., 2006). Briefly, after the indicated treatment cultures were fixed and MAP2 was immunolabeled. Thereafter MAP2-positive neurons were scored in three images taken at random in a fluorescence Zeiss microscopy with a 20 x objective and values were expressed as number of neurons per field.

For both methods, quantitative determinations were performed in a treatment-blind condition.

Dendritic degeneration and neuronal dystrophy

Dendritic morphology was evaluated in MAP-2 immunofluorescently labeled cultures. In each experimental condition three random images were taken per well using a Zeiss Axiovert inverted microscope with a 20 X objective. Image analysis was performed using FIJI software. For total MAP-2 fluorescent intensity and estimation of dendritic length images were equally processed. Briefly, background was subtracted, a threshold was applied and fluorescent intensity was obtained. Dendritic length was estimated after applying the skeletonize plugin on binary images. Assessment of dystrophic neurons was performed by analyzing neuronal morphology in MAP-2 fluorescent images. Neurons having abnormally short dendrites (shorter than two somas) or a single straight and unbranched dendrite or aberrantly tortuous and short dendrites were categorized as dystrophic. All experiments were analyzed in an experimental-blind condition.

Analysis of phosphorylated tau

Tau phosphorylation was evaluated in cultures immunofluorescently labeled with monoclonal antibody PHF-1 (Greenberg et al., 1992). In each experimental condition three random images were taken per well using a Zeiss Axiovert inverted microscope with a 20 X objective. Image analysis was performed using FIJI software. Phosphorylated tau missorting was determined by scoring neurons with PHF-1-positive somas and by assessing PHF-1 fluorescence intensity in somas. Briefly, background was subtracted, a threshold was applied and fluorescent intensity was obtained on the whole image (total PHF-1 fluorescence) or on a ROI in the cell somas (PHF-1 fluorescence in soma). In addition, PHF-1-positive somas were scored by visual inspection and expressed as percentage of total somas.

Quantification of synaptophysin puncta

Neuronal cultures were immunofluorescently labeled with anti-synaptophysin and anti-PSD95 antibodies. For each experimental condition confocal images were taken in an Olympus FV1000 Spectral microscope with a PLAPON 60X Oil objective (1.42 NA). For quantitative assessment of synaptic puncta, the synaptophysin channel alone was used and processed with the FIJI software. Briefly, background was subtracted, a threshold was applied and an automatic count was obtained from particles between 2 and 10 pixels of size.

Intra-dorsal-hippocampal (dHIP) Injections

Mice were prepared for the intra-dorsal-hippocampal injections of vehicle or drug solutions 48 h before training, so that a minimum of time was necessary for injection as previously described (Boccia et al., 2007; Boccia et al., 2004; Boccia et al., 2006; Krawczyk et al., 2016). The preliminary surgery consisted of an incision of the scalp. Two holes were drilled in the skull without perforating the brain, at the following stereotaxic coordinates AP: 1.90 mm posterior to

bregma, L/R + 1.50 mm from the midsagital suture and DV: 1.50 mm from a flat skull surface (Franklin and Paxinos, 1997), in order to bilaterally infuse the drugs after recovery. The skull was covered with bone wax and the mouse was returned to its home cage. Injections lasted 90 s and were driven by hand through a 30-gauge blunt stainless steel needle attached to a 5.00 µl Hamilton syringe with PE-10 tubing. The volume of each dHIP infusion was 0.50 µl. The accuracy of dHIP injections was determined by histological determination of the needle position on an animal-by-animal basis. For this purpose, the brains of injected animals were dissected, fixed in 4% paraformaldehyde/buffer phosphate saline, and stored in 30% sucrose. They were then cut into 200 µm coronal sections with a vibratome. The deepest position of the needle was superimposed on serial coronal maps (Franklin and Paxinos, 1997). Finally, infusion accuracy was verified with a magnifying glass. Animals were excluded from the statistical analysis if the infusions were beyond the intended area.

Novel object recognition task

The novel object recognition tasks was performed as previously described (Feld et al., 2014). Briefly, it consisted of a sample phase (training) and a testing phase. Before training, all mice were handled 5 min daily for 3 d and were habituated to the experimental arena for 2 consecutive days (10 and 15 min each) in the absence of objects. The experimental arena was a white rectangular open field (30 × 23 × 21.50 cm) bedded with sawdust. During the sample phase, mice were placed in the experimental arena with two objects (25-mL beakers, 3.0 cm diameter × 5.0 cm height; large blue Lego blocks, 3.0 × 3.0 × 1.8 cm) and were allowed to explore for 15 min. The objects were cleaned with ethanol 70% between trials to make sure no olfactory cues were present. Long-term memory was tested 24 h after training. During retention test, mice explored the experimental arena for 5 min in the presence of one familiar and one novel object. The novel objects were counterbalanced in all experiments. Sample and testing trials were videotaped and analyzed by individuals blind to the treatment condition and the

genotype of subjects. Videos were used to estimate the exploration time of novel and familiar objects. A mouse was scored as exploring an object when its head was oriented toward the object within a distance of 1 cm or when the nose was touching the object. The relative exploration time was recorded and expressed by a discrimination index (D.I.= $[t_{novel} - t_{familiar}] / [t_{novel} + t_{familiar}]$). Mean exploration times were calculated and the discrimination indexes between groups were compared.

Statistical analysis

Experiments were performed at least in triplicate and independently replicated 2-4 times with similar results. Experimental data were statistically analyzed by using one-way analysis of variance (ANOVA) followed by Tukey HSD post hoc test. Results are presented as means ± SEM. Frequency analysis was performed with non-parametric $\chi 2$ test.

Results

Aβ deposition enhances APP and Go interaction in dystrophic neurites

To characterize the effect of Aβ-deposition on the subcellular distribution and interaction of APP and Go proteins in mature hippocampal neurons (10-14 DIV), we performed immunofluorescence and confocal microscopy. Reminiscent to AD pathology in human brain (Cras et al., 1991), treatment with Aβ promoted a dramatic accumulation of APP in dystrophic neurites surrounding Aβ deposits (Supplementary Figure 1). Monoclonal antibodies A2 and Y188 were used to label Goα and the C-terminal domain of APP, respectively. In vehicle-treated neurons (control) Goα distributed homogeneously throughout the cell membrane of soma and neurites. Treatment with Aβ enhanced co-localization of APP and Goα around Aβ deposits (Figure 1A). In control cultures APP and Goα co-localization was 82.4 ± 0.07 % and Aβ treatment significantly increases APP and Goα co-localization to 92.4 ± 0.07% in neurites adjacent to Aβ-

deposits, while in neurites distant from the fibrils co-localization was similar to control (76.3 ± 0.1 %) (ANOVA F(2, 61)=5,5728, p=0.005). To analyze interaction of APP-holoprotein with Goα subunit we performed co-immunoprecipitation assay. HEK293 cells co-transfected with plasmid encoding for Goα subunit of heterotrimeric Go protein together with human neuronal APP isoform (695 aa) or an empty vector (ev). Supplementary Figure 2 depicts immunoprecipitaion experiments showing that overexpression of APP dramatically enhances co-immunoprecipitation of Goα with holo-APP. Specificity of co-immunoprecipitation of holo-APP and Goα was demonstrated by using N- and C-terminal APP antibodies and by co-precipitating holo-APP with polyclonal antibody K20 specific for Goα.

To ascertain if Aβ deposition effectively enhances endogenous APP and Goα interaction in neurons, we performed fluorescence resonance energy transfer (FRET) analysis in mature hippocampal cultures immuno-labeled with antibodies Y188 and A2 (Figure 1A). FRET microscopy allows to study interaction between fluorescently labeled proteins by providing an accurate measure of the variations in the proximity (<100 Å) between fluorophores. We assessed FRET employing the acceptor (APP C-terminal domain Y188/Alexa Fluor 568) photobleaching method, which dequenches the donor (Goα A2/Alexa Fluor 488) (Figure 1B). Quantitative analysis of FRET signals across different segments of neurites in vehicle-treated control cultures revealed a mean FRET efficiency (EM) of 0.037 ± 0.006. Treatment with Aβ fibrils significantly enhanced FRET in dystrophic neurites to EM 0.140 ± 0.030, which represent a 378 ± 81 % increase (ANOVA F(2, 110)=7.5337, p=0.0008, Figure 1C). Non-parametric statistical analysis showed that Aβ significantly increased the percentage of neurites with higher FRET values (X^2(6)=30.04; p<0.0001; Figure 1D). Excluding APP Y188 antibody during immunolabeling in Aβ-treated cultures reduced EM to a negligible 0.012 ± 0.004 and dramatically increased the percentage of neurites with low FRET values, ruling-out nonspecific association of fluorophores in Aβ-treated cultures (Figure 1D). To further confirm the enhancement of APP and Goα interaction

by Aβ deposition, we performed FRET in a different configuration. Hippocampal neurons were transfected with plasmid encoding for human APP C-terminally tagged with the yellow fluorescent protein (APP-YFP) and endogenous Goα was immuno-labeled with monoclonal A2 antibody followed by Alexa 568 secondary antibody. As shown in Supplementary Figure 3 quantitative analysis of FRET confirmed that Aβ induced a highly significant increase in EM (ANOVA $F(2, 36)=29.761$; $p=0.0000$) increasing the percentage of neurites with higher FRET values ($X^2(6)=52.11$; $p<0.0001$). These observations indicate that endogenous APP and Goα physically interact in intact mature hippocampal neurons, and Aβ deposition dramatically enhances APP-Goα interaction in dystrophic neurites.

APP overexpression sensitizes neurons to Aβ-toxicity through Go protein Gβγ complex signaling activation

To study the signaling mechanism by which APP/Go might trigger Aβ neurotoxicity we employed a previously reported assay that allows studying APP-dependent signaling involved in Aβ-toxicity (Sola Vigo et al., 2009). Hippocampal cultures (2-3 DIV) were co-transfected with plasmids encoding YFP together with neuronal human APP or an empty vector (ev) as control. Then, the cultures were treated with vehicle (control) or Aβ and after 6-8h viability was assessed by scoring YPF-positive neurons with healthy morphological appearance of soma and neurites. In full agreement with our previous report (Sola Vigo et al., 2009), we found that viability in control ev-transfected neurons were not affected after this short period of Aβ treatment (Figure 2A). On the contrary, in neurons overexpressing APP, Aβ treatment induced a significant 22.8±6.1% reduction in neuronal viability, which corresponds to APP-dependent toxicity of Aβ. Treatment with Pertussis toxin (PTX) abrogated APP-dependent toxicity of Aβ which was restored by expression of a PTX-insensitive mutant of Gαo (iPTX-Go) (ANOVA $F(3, 74)=13.143$; $p=0.00000$;

Figure 2A). To examine whether activation of Goα subunit per se mediate Aβ-neurotoxicity in hippocampal cultures we over-expressed the constitutively-activated GTPase-deficient form of Goα protein (Goα-QL) and neuronal viability was scored at various time-points. Neuronal viability was not significantly affected in neurons overexpressing Goα-QL (ANOVA (5, 39)=2,2433, p=0.069; data not shown), suggesting that direct signaling through Goα subunit per se does not promote neuronal degeneration. On the other hand, we found that a stepwise-increasing expression of wtGoα inhibited APP-dependent Aβ-toxicity in a dose-dependent manner (ANOVA F(4,68)=8.8534, p=0.00001; Figure 2B). Moreover, transfection with the β adrenergic receptor kinase C-terminal peptide (βARK), a universal antagonist of Gβγ complex (Ramirez et al., 2016), significantly abrogated APP-mediated toxicity of Aβ (ANOVA F(3, 26)=7.9760, p=0.0062; Figure 2C). To further analyze the participation of Gβγ complex in APP-mediated Aβ-toxicity, we examined the effect of gallein, a small molecule that specifically binds to Gβγ complex preventing its interaction with downstream signaling effectors (Lehmann et al., 2008; Seneviratne et al., 2011). As expected, Aβ treatment did not altered viability in control ev-transfected cultures while in APP-overexpressing neurons viability was significantly reduced to 60.9±9.0%. Gallein completely abrogated this toxic effect (ANOVA F(3, 24)=4.6461, p=0.01; Figure 2D), indicating that signaling through Gβγ complex rather than Goα subunit mediates APP-dependent toxicity of Aβ.

Go protein Gβγ complex signaling mediates Aβ-induced neurodegeneration in *in vitro* model of Alzheimer´s disease

Misleading interpretations of the mechanisms of Aβ-toxicity might arise from experimental approaches exclusively based on APP-overexpression (Saito et al., 2014; Saito et al., 2016). Thus, we analyzed the involvement of the Gβγ complex activation in Aβ-toxicity in 10-14 DIV

hippocampal neurons expressing endogenous protein levels. After 24 and 48 h of Aβ treatment neuronal viability was reduced to 67.3 ± 14.3 % and 46.3 ± 4.11 %, respectively. Notably, gallein dramatically delayed Aβ-induced neuronal loss preserving viability to 89.9 ± 4.81 and 79.03 ± 9.31 % after 24 and 48 h, respectively (ANOVA F(5, 17)=23,099, p= 0.0000; Figure 3A and 3B). The protective effect of gallein on Aβ-toxicity was also observed on dendritic morphology as determined by MAP2 fluorescence (ANOVA F(5, 16)=9.4688; P=0.00024; Figure 3D), increased dendritic length (ANOVA F(5, 16)=21,767, p=0.0000; Figure 3E) and reduced number of dystrophic neurons (ANOVA F(5, 18)=34,248, p=0.0000, Figure 3C).

We then analyzed the involvement of Go protein Gβγ complex signaling in Aβ-induced tau-phosphorylation. Hippocampal cultures were treated with Aβ and tau phosphorylation was assessed after 48 h by immunofluorescence with monoclonal antibody PHF1 that selectively recognizes a tau epitope phosphorylated at Ser-396/Ser404 in PHFs (Greenberg et al., 1992; Lang et al., 1992). Treatment with Aβ led to a series of pathologic changes in axonal morphology, including increased tortuosity and a marked reduction in axonal network density (Figure 4A). These changes were accompanied by an increased intensity in PHF-1 fluorescence and abnormal immunostaining of somatodendritic compartment (Figure 4A). Gallein treatment counteracted the pathological effects of Aβ improving axonal appearance, reducing the number of PHF-1-positive somas (ANOVA F(2, 27)=28.568; p=0.000; Figure 4B), decreased somatic PHF-1 fluorescence intensity (ANOVA F(2, 72)=86.847; p=0.000, Figure 4C) as well as the total mean fluorescent intensity (ANOVA F(2, 242)=5.8852, p=0.0083; Figure 4D).

Next we examined whether morphological protection of axons and dendrites by gallein preserves structural synaptic connectivity in Aβ-treated cultures. We characterized structural synaptic contacts in mature hippocampal cultures by immunofluorescence with antibodies against PSD95 and synaptophysin. Confocal microscopy images showed that near all presynaptic synaptophysin puncta were juxtaposed to a postsynaptic PSD95 cluster, indicating axonal and

dendritic functional synaptic interaction (Figure 5). Based on this observation we scored synaptophysin puncta as a reliable determination of structural synaptic contacts in the cultures. Quantitative image analysis showed that treatment with Aβ led to a dramatic reduction in the number of synaptophysin puncta while inhibition of Gβγ complex signaling by gallein significantly prevented this toxic effect (ANOVA (3, 36)=12.223; p=0.00001; Figure 5). These observations suggest that inhibition of Gβγ complex signaling by gallein exerts a broad neuroprotective effect on Aβ-toxicity.

p38 MAPK is a downstream effector of Go protein Gβγ complex signaling involved in Aβ-induced neurodegeneration

To search for downstream effectors of APP/ Go protein Gβγ complex signaling of Aβ-toxicity we focused on mitogen activated protein kinases (MAPKs) which are well known downstream effectors of Gβγ complex of G proteins (Marinissen and Gutkind, 2001). Hippocampal neurons (2-3 DIV) were co-transfected with the plasmids encoding YFP and APP or empty vector (ev) as control. After transfection, cultures were treated with vehicle (control) or the specific pharmacological inhibitors of c-Jun N-terminal kinase (JNK, SP600125); p38-MAPK (SB203580), and extracellular-regulated kinase (ERK, PD98059). Also, the specific inhibitor of P21-activated kinase 3 (PAK3, IPA3) was analyzed since this kinase was previously implicated in neuronal toxicity elicited by FAD-APP overexpression (McPhie et al., 2003). One hour later d Aβ was added and healthy YFP-positive neurons were scored after 8h of treatment. As expected, Aβ did not induce toxicity to ev-transfected neurons, but it promoted a significant reduction in neuronal viability to 66.7 ± 3.1 % in APP-transfected neurons. Inhibition of p38-MAPK in Aβ-treated cultures restored viability to control levels, while inhibitors of JNK, ERK or PAK3 were not effective in these experimental conditions (ANOVA F(11, 305)=12.180; p=0.0000; Figure 6A). Neither p38-MAPK-, JNK-, ERK-, or PAK3-inhibitors per se affected neuronal viability in vehicle-

treated ev-YFP or APP-YFP cultures (data not shown). These experiments suggest that p38-MAPK activation mediates APP-dependent toxicity of Aβ.

Next, we aim to confirm that in non-transfected neurons p38-MAPK is effectively activated by Aβ downstream of Gβγ complex signaling. Mature hippocampal cultures were treated with vehicle (control) or Aβ without or with SB203580 or gallein. After 3 h, cultures were homogenized and cell lysates were analyzed by western blot with antibodies that recognize p38-MAPK irrespective of its phosphorylation state (total p38-MAPK) or that selectively recognizes activated p38-MAPK, phosphorylated at Thr180/Tyr182 (P-p38). In control cultures levels of P-p38 were readily detected and treatment with Aβ enhanced p38-MAPK-activation after 3 h without altering total p38-MAPK levels (Figure 6B). The enhanced activation of p38-MAPK by Aβ was not longer appreciated after 24 h of treatment (data not shown). Significantly, SB203580 and gallein prevented Aβ-triggered p38-MAPK phosphorylation observed at 3 h post-treatment (ANOVA $F(6, 21)=10.008$; $p=0.00003$, Figure 6B). These data provide evidences that p38-MAPK is activated by Aβ and its activation requires Gβγ complex signaling.

To confirm that p38-MAPK activation is involved in Aβ-induced degeneration in mature neurons expressing endogenous protein levels, hippocampal cultures were treated for 24 h with vehicle or Aβ alone or in the presence of SB203580. Thereafter, somatodendritic and axonal compartments were respectively labeled with MAP2 and PHF-1 antibodies and Aβ-induced neuronal degeneration was assessed by scoring dystrophic neurons with collapsed dendrites and PHF-1 positive somas. As expected, Aβ significant increased the number of dystrophic neurons with collapsed dendrites and neurons with PHF-1 positive somas. Inhibition of p38-MAPK activity with SB203580 significantly reduced the dendritic dystrophy (ANOVA $F(3, 44)=177,63$; $p=0.000$; Figure 6C), the intensity of PHF-1 fluorescence in somas (ANOVA $F(3, 44)=25.655$; $p=0.0000$; Figure 6D) as well as number of neurons with positive PHF-1 fluorescence in the somas induced by Aβ treatment (ANOVA $F(3, 65)=16.733$; $p=0.000$; Figure 6E). Altogether, experiments indicate

that p38-MAPK is an effector downstream of APP/Go protein Gβγ complex involved in Aβ-induced neurodegeneration.

Pharmacological inhibition of Gβγ complex signaling by gallein restores memory performance in an *in vivo* model of Alzheimer´s disease

Transgenic mice models of AD, including the triple-transgenic 3xTg-AD mice, have been extensively used to study Aβ-dependent mechanisms of synaptic and cognitive impairment. At 6 months of age, 3xTg-AD mice develop early signs of Aβ pathology accompanied by hippocampal synaptic dysfunction and long-term potentiation deficits (Oddo et al., 2003). We showed that 3xTg-AD mice developed age-dependent long term memory deficits between by 5-6 months in a novel object recognition (NOR) task, which correlates with early Aβ aggregation patterns according to the mice's age and brain region (Feld et al., 2014). Therefore, we tested whether enhanced activity of Gβγ complex signaling in the hippocampus of the 3xTg-AD mice might contribute to impaired memory recognition. Vehicle (control) or gallein were injected in the dorsal hippocampus (dHIP) 90 minutes before training in the NOR task and mice were tested for retention after 24 h (Figure 7A and C). Statistical analysis demonstrated treatment-related significant differences (ANOVA $F(2,15)$ 8.7460, $p=0.00304$). Tukey post-hoc analysis revealed a significant impairment in memory retention in vehicle-treated 3xTgAD mice compared to vehicle-treated wild-type (Figure 7B). Remarkably, gallein-treated 3xTgAD mice spent significantly more time exploring the novel object than the vehicle-treated 3xTgAD animals. This observation shows that in the 3xTg-AD mice intra-hippocampal inhibition of Gβγ-complex signaling by gallein improved either memory acquisition, consolidation or both.

Discussion

Elucidating the mechanism by which toxic Aβ assemblies induce neuronal dysfunction and memory impairment is instrumental for developing rational interventions for AD. In particular, clarifying the mechanism by which APP is entailed in Aβ-toxicity might help to reveal how Aβ deposition and neuronal dysfunction spread in AD brain.

In the present study, employing rat primary hippocampal cultures we found that Aβ deposition enhances interaction of APP with Goα protein in dystrophic neurites. We confirmed that APP overexpression rendered hippocampal neurons vulnerable to Aβ-toxicity and demonstrated that this effect was mediated by Go-Gβγ complex signaling and p38-MAPK activation. We discovered that gallein significantly diminished Aβ-induced degeneration in both APP-overexpressing neurons and mature hippocampal neurons expressing endogenous protein levels. The protective effect of gallein against Aβ toxicity in mature neurons was robust and extended to several pathologic markers characteristic of AD, including p38-MAPK activation, mislocalization of abnormally phosphorylated tau into the somatodendritic compartment, dystrophic degeneration of axons and dendrites, loss of synapses and neuronal cell death. Moreover, in the 3xTg-AD mice model of AD we showed that inhibition of Gβγ complex signaling by gallein reversed the memory deficit that arises in early stages of Aβ-pathology. Altogether, our data indicate that Aβ-toxicity is mediated by enhanced activity of Gβγ complex likely due to sustained APP and Go protein activation.

Previous studies showed that APP binds Aβ peptides, including endogenously secreted Aβ species (Cras et al., 1991; Fogel et al., 2014) and pathological assemblies of the peptide (Kedikian et al., 2010; Lorenzo et al., 2000; Shaked et al., 2006; Van Nostrand et al., 2002). In B103 cell line it was suggested that Aβ reduces co-localization of APP and Go (Shaked et al., 2009). On the contrary, in primary neurons interaction of APP with Aβ (physiological and pathological species) promotes cell surface accumulation/multimerization of APP and activation of Go signaling (Fogel et al., 2014; Heredia et al., 2004; Sola Vigo et al., 2009). Physiological Aβ

species have been associated to normal synaptic activity (Abramov et al., 2009; Fogel et al., 2014), while pathological Aβ assemblies cause aberrant activity in neuronal circuits and neurodegeneration (Hartley et al., 1999). The mechanisms by which APP might contribute to the different biological effect elicited by distinct Aβ species remain poorly understood. It is possible that accumulation of Aβ and/or its ineffective clearance in AD brain might pathologically sustain their biological activity causing neuronal toxicity. Here we showed that, in primary neurons, deposition of Aβ enhanced accumulation and interaction of APP with Go in dystrophic neurites, even days after treatment. We used C- and N-terminal antibodies against APP to confirm that holo-APP and Goα co-immunoprecipitates, suggesting direct interaction of these proteins. Coincidently, it was reported that APP co-immunoprecipitates with heterotrimeric Go protein in rat and human brain homogenates (Ramaker et al., 2013; Shaked et al., 2009). We confirmed that deposition of Aβ enhanced APP/Goα interaction by performing FRET analysis under different configuration of fluorophores and, particularly, in intact mature hippocampal neurons expressing endogenous protein levels. This makes unlikely that APP-Goα interaction might occur artifactually after cell lysis (in co-ip experiments) or as a consequence of APP and/or Goα overexpression in transfected cells. Furthermore, our FRET data indicate that APP/Goα interaction was particularly robust in dystrophic neurites around Aβ deposits, suggesting that Aβ aggregates persistently stimulate APP/Go protein triggering degeneration.

Increasing evidence support an evolutionary conserved role of APP-family members as atypical GPCR that contributes to neuronal plasticity though Go signaling (Copenhaver and Kogel, 2017). The pathological involvement of APP/Go signaling in Aβ-toxicity was previously reported by overexpressing diverse deletion-mutant forms of APP and/or subunits of G proteins in primary neurons (Sola Vigo et al., 2009) and also in the neuronal cell line B103 (Shaked et al., 2009). In addition, reports from several groups show that, independent of Aβ treatment, overexpression of FAD-APP per se promotes neuronal apoptosis by activating Go signaling in

different cell lines (Giambarella et al., 1997; Yamatsuji et al., 1996) and in primary neurons (McPhie et al., 2003; Niikura et al., 2004), suggesting that FAD-APP overexpression can constitutively activate Go (Okamoto et al., 1996). In our experimental conditions we showed that overexpression of wild-type APP in hippocampal neurons did not induced toxicity per se, but selectively enhanced neuronal vulnerability to aggregated Aβ peptides by a Go protein dependent mechanism (Figure 3A ; see also Sola Vigo et al., 2009). Here we showed that Aβ-toxicity in APP-transfected neurons was abrogated by overexpressing the Goα subunit of Go protein or the C-terminus of the β adrenergic receptor kinase (βARK), which are universally used as Gβγ complex-scavenger (Ramirez et al., 2016). Furthermore, gallein inhibited Aβ-toxicity in APP-transfected neurons as well as in non-transfected mature hippocampal cultures, showing that enhanced Gβγ complex signaling contributes to Aβ-induced degeneration likely by APP-Go protein activation.

Tau protein plays a crucial role in Aβ-induced neuronal dysfunction and death (Ittner et al., 2010; Rapoport et al., 2002; Roberson et al., 2007). Here show that gallein effectively prevented Aβ-induced tau hyperphosphorylation and mislocalization into the somatodendritic compartment. We previously demonstrated that Aβ fibrils increases tau phosphorylation at the PHF-1 epitope in rat and human cultured neurons, which is accompanied by missorting of tau to somatodendritic compartment and impaired capacity of microtubule binding (Busciglio et al., 1995). Tau can be phosphorylated by several protein kinases, including p38-MAPK which can directly phosphorylate tau at Serines 396 and 404 (Reynolds et al., 2000) which are the phosphorylated residues required for epitope-recognition by the PHF1 antibody. Previous reports showed activation of p38-MAPK by Aβ (Giraldo et al., 2014) and increased p38-MAPK activity in AD (Zhu et al., 2000). Here we extended these observations by showing that Aβ-triggered p38-MAPK activation was inhibited by SB203580 and by gallein. Moreover, SB203580 and gallein effectively reduced Aβ-induced degeneration in primary neurons overexpressing APP as well as in neurons expressing

endogenous protein levels. These experiments provide further evidence that p38-MAPK is a downstream effector of APP/Go protein Gβγ complex signaling involved in Aβ-toxicity and tau phosphorylation.

Synaptic loss is another pathological feature of AD that correlates with clinical symptoms (Scheff et al., 2015). Here we showed that Aβ treatment dramatically reduced synaptophysin/PSD95 clusters in mature hippocampal cultures, which was prevented by inhibition of Gβγ complex signaling by gallein. This observation suggests that Aβ deposition triggers pathologic activation of Go protein Gβγ complex signaling resulting in synapse loss. Our experiments were not designed to determine whether Aβ-triggered synaptic loss was due to a direct effect on pre/postsynaptic components or indirectly as a consequence of neuritic retraction and dystrophy. Interestingly, it was recently demonstrated that dendritic dystrophy per se might functionally affect input to action potential conversion, causing hyperexcitability and network dysfunction in AD mice model (Siskova et al., 2014). Therefore, the strong *in vitro* effect of gallein preventing Aβ-induced dystrophy and synaptic loss suggests its potential as a therapeutic agent for Aβ-related cognitive impairment. We used the 3xTg-AD mice and NOR task to assess the effect of gallein on long term memory performance. The NOR task is a very sensitive declarative memory task which is not supposed to involve anxiety or unspecific effects on sensory systems (Dere et al., 2007) and is strongly dependent on the activity of the dorsal hippocampus. We found that in 6 months old 3xTg-AD mice an intra-hippocampal injection of gallein short before training was sufficient to reverse memory impairment. This observation shows that enhanced Gβγ complex signaling in the dorsal hippocampus might contribute to impairment in memory processing in 3xTg-AD mice, and therefore the local application of gallein restored functional processing of memory recognition. This behavioral observation, together with our *in vitro* data suggest that toxic Aβ assemblies trigger pathologic and sustained APP/Go protein Gβγ complex signaling leading to synaptic dysfunction and to cognitive impairment in the 3xTg-AD mice.

Accumulation of Aβ in the brain precedes by years neurological symptoms and clinical diagnose of AD (Bateman et al., 2012). Therefore, early detection of Aβ in the brain with new diagnostics methods must be complemented with effective therapies for halting Aβ-induced degeneration. Our data provide new evidence for the participation of APP as an unconventional GPCR playing a pivotal role in Aβ-toxicity, and revealed that Go protein Gβγ complex might function as a signaling hub mediating neuronal dysfunction and degeneration triggered by toxic Aβ assemblies. Considering that GPCR have been the target of >50% of the pharmaceutical development on the market (Flower, 1999), our data suggest that APP/Go protein Gβγ complex might have value for AD therapeutic development.

Conclusion

Our results show that toxic Aβ assemblies trigger pathologically sustained APP/Go protein Gβγ complex signaling that causes neuronal degeneration in hippocampal neurons and cognitive dysfunction in the 3xTg-AD mice. Therefore APP/Go protein Gβγ complex might be a target for developing therapeutic interventions to halt Aβ-degeneration in Alzheimer´s disease based on a disease mechanism.

Acknowledgements

We gratefully acknowledge Gonzalo Quassollo for his technical assistance in FRET microscopy, and Andrea Pellegrini for her technical assistance in tissue culture.

Formatting of funding sources

This work was supported by grants from ANPCyT PICT 2014-3155 and FONARSEC-SB-PBIT 2013-09 to A.L., ANPCyT PICT 2014-1768 to A.B.; CONICET PIP 11220150100954CO to GFP, ANPCyT PICT 2013-0375, CONICET PIP 1122013010045 and grant UBACyT 2014–2017 – 20020130100881BA to M.B. Alzheimer´s Association New Investigator Research Grant to Promote Diversity NIRGD-11-206379 to GFP. EAB, GFP, MMB and AL are career members of CONICET.

References

Abramov, E., Dolev, I., Fogel, H., Ciccotosto, G.D., Ruff, E., Slutsky, I., 2009. Amyloid-beta as a positive endogenous regulator of release probability at hippocampal synapses. Nat Neurosci 12(12), 1567-1576.

Bateman, R.J., Xiong, C., Benzinger, T.L., Fagan, A.M., Goate, A., Fox, N.C., Marcus, D.S., Cairns, N.J., Xie, X., Blazey, T.M., Holtzman, D.M., Santacruz, A., Buckles, V., Oliver, A., Moulder, K., Aisen, P.S., Ghetti, B., Klunk, W.E., McDade, E., Martins, R.N., Masters, C.L., Mayeux, R., Ringman, J.M., Rossor, M.N., Schofield, P.R., Sperling, R.A., Salloway, S., Morris, J.C., 2012. Clinical and biomarker changes in dominantly inherited Alzheimer's disease. N Engl J Med 367(9), 795-804.

Bignante, E.A., Heredia, F., Morfini, G., Lorenzo, A., 2013. Amyloid beta precursor protein as a molecular target for amyloid beta--induced neuronal degeneration in Alzheimer's disease. Neurobiol Aging 34(11), 2525-2537.

Boccia, M., Freudenthal, R., Blake, M., de la Fuente, V., Acosta, G., Baratti, C., Romano, A., 2007. Activation of hippocampal nuclear factor-kappa B by retrieval is required for memory reconsolidation. J Neurosci 27(49), 13436-13445.

Boccia, M.M., Acosta, G.B., Blake, M.G., Baratti, C.M., 2004. Memory consolidation and reconsolidation of an inhibitory avoidance response in mice: effects of i.c.v. injections of hemicholinium-3. Neuroscience 124(4), 735-741.

Boccia, M.M., Blake, M.G., Acosta, G.B., Baratti, C.M., 2006. Post-retrieval effects of icv infusions of hemicholinium in mice are dependent on the age of the original memory. Learn Mem 13(3), 376-381.

Busciglio, J., Lorenzo, A., Yeh, J., Yankner, B.A., 1995. Beta-amyloid fibrils induce tau phosphorylation and loss of microtubule binding. Neuron 14(4), 879-888.

Cirrito, J.R., Yamada, K.A., Finn, M.B., Sloviter, R.S., Bales, K.R., May, P.C., Schoepp, D.D., Paul, S.M., Mennerick, S., Holtzman, D.M., 2005. Synaptic activity regulates interstitial fluid amyloid-beta levels in vivo. Neuron 48(6), 913-922.

Copenhaver, P.F., Kogel, D., 2017. Role of APP Interactions with Heterotrimeric G Proteins: Physiological Functions and Pathological Consequences. Front Mol Neurosci 10, 3.

Cras, P., Kawai, M., Lowery, D., Gonzalez-DeWhitt, P., Greenberg, B., Perry, G., 1991. Senile plaque neurites in Alzheimer disease accumulate amyloid precursor protein. Proc Natl Acad Sci U S A 88(17), 7552-7556.

Dahlgren, K.N., Manelli, A.M., Stine, W.B., Jr., Baker, L.K., Krafft, G.A., LaDu, M.J., 2002. Oligomeric and fibrillar species of amyloid-beta peptides differentially affect neuronal viability. J Biol Chem 277(35), 32046-32053.

Dere, E., Huston, J.P., De Souza Silva, M.A., 2007. The pharmacology, neuroanatomy and neurogenetics of one-trial object recognition in rodents. Neurosci Biobehav Rev 31(5), 673-704.

Deshpande, A., Mina, E., Glabe, C., Busciglio, J., 2006. Different conformations of amyloid beta induce neurotoxicity by distinct mechanisms in human cortical neurons. J Neurosci 26(22), 6011-6018.

Feld, M., Krawczyk, M.C., Sol Fustinana, M., Blake, M.G., Baratti, C.M., Romano, A., Boccia, M.M., 2014. Decrease of ERK/MAPK overactivation in prefrontal cortex reverses early memory deficit in a mouse model of Alzheimer's disease. J Alzheimers Dis 40(1), 69-82.

Flower, D.R., 1999. Modelling G-protein-coupled receptors for drug design. Biochim Biophys Acta 1422(3), 207-234.

Fogel, H., Frere, S., Segev, O., Bharill, S., Shapira, I., Gazit, N., O'Malley, T., Slomowitz, E., Berdichevsky, Y., Walsh, D.M., Isacoff, E.Y., Hirsch, J.A., Slutsky, I., 2014. APP homodimers transduce an amyloid-beta-mediated increase in release probability at excitatory synapses. Cell Rep 7(5), 1560-1576.

Franklin, K.B.J., Paxinos, G., 1997. The Mouse Brain in Stereotaxic Coordinates. . San Diego: Academic Press.

Giambarella, U., Yamatsuji, T., Okamoto, T., Matsui, T., Ikezu, T., Murayama, Y., Levine, M.A., Katz, A., Gautam, N., Nishimoto, I., 1997. G protein beta-gamma complex-mediated apoptosis by familial Alzheimer's disease mutant of APP. EMBO J 16(16), 4897-4907.

Giraldo, E., Lloret, A., Fuchsberger, T., Vina, J., 2014. Abeta and tau toxicities in Alzheimer's are linked via oxidative stress-induced p38 activation: protective role of vitamin E. Redox Biol 2, 873-877.

Greenberg, S.G., Davies, P., Schein, J.D., Binder, L.I., 1992. Hydrofluoric acid-treated tau PHF proteins display the same biochemical properties as normal tau. J Biol Chem 267(1), 564-569.

Hartley, D.M., Walsh, D.M., Ye, C.P., Diehl, T., Vasquez, S., Vassilev, P.M., Teplow, D.B., Selkoe, D.J., 1999. Protofibrillar intermediates of amyloid beta-protein induce acute electrophysiological changes and progressive neurotoxicity in cortical neurons. J Neurosci 19(20), 8876-8884.

Heredia, L., Helguera, P., de Olmos, S., Kedikian, G., Sola Vigo, F., LaFerla, F., Staufenbiel, M., de Olmos, J., Busciglio, J., Caceres, A., Lorenzo, A., 2006. Phosphorylation of actin-depolymerizing factor/cofilin by LIM-kinase mediates amyloid beta-induced degeneration: a potential mechanism of neuronal dystrophy in Alzheimer's disease. J Neurosci 26(24), 6533-6542.

Heredia, L., Lin, R., Vigo, F.S., Kedikian, G., Busciglio, J., Lorenzo, A., 2004. Deposition of amyloid fibrils promotes cell-surface accumulation of amyloid beta precursor protein. Neurobiol Dis 16(3), 617-629.

Ittner, L.M., Ke, Y.D., Delerue, F., Bi, M., Gladbach, A., van Eersel, J., Wolfing, H., Chieng, B.C., Christie, M.J., Napier, I.A., Eckert, A., Staufenbiel, M., Hardeman, E., Gotz, J., 2010. Dendritic function of tau mediates amyloid-beta toxicity in Alzheimer's disease mouse models. Cell 142(3), 387-397.

Kedikian, G., Heredia, F., Salvador, V.R., Raimunda, D., Isoardi, N., Heredia, L., Lorenzo, A., 2010. Secreted amyloid precursor protein and holo-APP bind amyloid beta through distinct domains eliciting different toxic responses on hippocampal neurons. J Neurosci Res 88(8), 1795-1803.

Krawczyk, M.C., Navarro, N., Blake, M.G., Romano, A., Feld, M., Boccia, M.M., 2016. Reconsolidation-induced memory persistence: Participation of late phase hippocampal ERK activation. Neurobiol Learn Mem 133, 79-88.

Lang, E., Szendrei, G.I., Lee, V.M., Otvos, L., Jr., 1992. Immunological and conformation characterization of a phosphorylated immunodominant epitope on the paired helical filaments found in Alzheimer's disease. Biochem Biophys Res Commun 187(2), 783-790.

Lehmann, D.M., Seneviratne, A.M., Smrcka, A.V., 2008. Small molecule disruption of G protein beta gamma subunit signaling inhibits neutrophil chemotaxis and inflammation. Mol Pharmacol 73(2), 410-418.

Lorenzo, A., Yuan, M., Zhang, Z., Paganetti, P.A., Sturchler-Pierrat, C., Staufenbiel, M., Mautino, J., Vigo, F.S., Sommer, B., Yankner, B.A., 2000. Amyloid beta interacts with the amyloid precursor protein: a potential toxic mechanism in Alzheimer's disease. Nat Neurosci 3(5), 460-464.

Marinissen, M.J., Gutkind, J.S., 2001. G-protein-coupled receptors and signaling networks: emerging paradigms. Trends Pharmacol Sci 22(7), 368-376.

McPhie, D.L., Coopersmith, R., Hines-Peralta, A., Chen, Y., Ivins, K.J., Manly, S.P., Kozlowski, M.R., Neve, K.A., Neve, R.L., 2003. DNA synthesis and neuronal apoptosis caused by familial Alzheimer disease mutants of the amyloid precursor protein are mediated by the p21 activated kinase PAK3. J Neurosci 23(17), 6914-6927.

Milosch, N., Tanriover, G., Kundu, A., Rami, A., Francois, J.C., Baumkotter, F., Weyer, S.W., Samanta, A., Jaschke, A., Brod, F., Buchholz, C.J., Kins, S., Behl, C., Muller, U.C., Kogel, D., 2014. Holo-APP and G-protein-mediated signaling are required for sAPPalpha-induced activation of the Akt survival pathway. Cell Death Dis 5, e1391.

Nelson, P.T., Alafuzoff, I., Bigio, E.H., Bouras, C., Braak, H., Cairns, N.J., Castellani, R.J., Crain, B.J., Davies, P., Del Tredici, K., Duyckaerts, C., Frosch, M.P., Haroutunian, V., Hof, P.R., Hulette, C.M., Hyman, B.T., Iwatsubo, T., Jellinger, K.A., Jicha, G.A., Kovari, E., Kukull, W.A., Leverenz,

J.B., Love, S., Mackenzie, I.R., Mann, D.M., Masliah, E., McKee, A.C., Montine, T.J., Morris, J.C., Schneider, J.A., Sonnen, J.A., Thal, D.R., Trojanowski, J.Q., Troncoso, J.C., Wisniewski, T., Woltjer, R.L., Beach, T.G., 2012. Correlation of Alzheimer disease neuropathologic changes with cognitive status: a review of the literature. J Neuropathol Exp Neurol 71(5), 362-381.

Niikura, T., Yamada, M., Chiba, T., Aiso, S., Matsuoka, M., Nishimoto, I., 2004. Characterization of V642I-AbetaPP-induced cytotoxicity in primary neurons. J Neurosci Res 77(1), 54-62.

Nishimoto, I., Okamoto, T., Matsuura, Y., Takahashi, S., Murayama, Y., Ogata, E., 1993. Alzheimer amyloid protein precursor complexes with brain GTP-binding protein G(o). Nature 362(6415), 75-79.

Oddo, S., Caccamo, A., Shepherd, J.D., Murphy, M.P., Golde, T.E., Kayed, R., Metherate, R., Mattson, M.P., Akbari, Y., LaFerla, F.M., 2003. Triple-transgenic model of Alzheimer's disease with plaques and tangles: intracellular Abeta and synaptic dysfunction. Neuron 39(3), 409-421.

Okamoto, T., Takeda, S., Giambarella, U., Murayama, Y., Matsui, T., Katada, T., Matsuura, Y., Nishimoto, I., 1996. Intrinsic signaling function of APP as a novel target of three V642 mutations linked to familial Alzheimer's disease. EMBO J 15(15), 3769-3777.

Patel, T.B., 2004. Single transmembrane spanning heterotrimeric g protein-coupled receptors and their signaling cascades. Pharmacol Rev 56(3), 371-385.

Ramaker, J.M., Swanson, T.L., Copenhaver, P.F., 2013. Amyloid precursor proteins interact with the heterotrimeric G protein Go in the control of neuronal migration. J Neurosci 33(24), 10165-10181.

Ramirez, V.T., Ramos-Fernandez, E., Henriquez, J.P., Lorenzo, A., Inestrosa, N.C., 2016. Wnt-5a/Frizzled9 Receptor Signaling through the Galphao-Gbetagamma Complex Regulates Dendritic Spine Formation. J Biol Chem 291(36), 19092-19107.

Rapoport, M., Dawson, H.N., Binder, L.I., Vitek, M.P., Ferreira, A., 2002. Tau is essential to beta -amyloid-induced neurotoxicity. Proc Natl Acad Sci U S A 99(9), 6364-6369.

Reynolds, C.H., Betts, J.C., Blackstock, W.P., Nebreda, A.R., Anderton, B.H., 2000. Phosphorylation sites on tau identified by nanoelectrospray mass spectrometry: differences in vitro between the mitogen-activated protein kinases ERK2, c-Jun N-terminal kinase and P38, and glycogen synthase kinase-3beta. J Neurochem 74(4), 1587-1595.

Roberson, E.D., Scearce-Levie, K., Palop, J.J., Yan, F., Cheng, I.H., Wu, T., Gerstein, H., Yu, G.Q., Mucke, L., 2007. Reducing endogenous tau ameliorates amyloid beta-induced deficits in an Alzheimer's disease mouse model. Science 316(5825), 750-754.

Saito, T., Matsuba, Y., Mihira, N., Takano, J., Nilsson, P., Itohara, S., Iwata, N., Saido, T.C., 2014. Single App knock-in mouse models of Alzheimer's disease. Nat Neurosci 17(5), 661-663.

Saito, T., Matsuba, Y., Yamazaki, N., Hashimoto, S., Saido, T.C., 2016. Calpain Activation in Alzheimer's Model Mice Is an Artifact of APP and Presenilin Overexpression. J Neurosci 36(38), 9933-9936.

Scheff, S.W., Price, D.A., Ansari, M.A., Roberts, K.N., Schmitt, F.A., Ikonomovic, M.D., Mufson, E.J., 2015. Synaptic change in the posterior cingulate gyrus in the progression of Alzheimer's disease. J Alzheimers Dis 43(3), 1073-1090.

Selkoe, D.J., Hardy, J., 2016. The amyloid hypothesis of Alzheimer's disease at 25 years. EMBO Mol Med 8(6), 595-608.

Seneviratne, A.M., Burroughs, M., Giralt, E., Smrcka, A.V., 2011. Direct-reversible binding of small molecules to G protein betagamma subunits. Biochim Biophys Acta 1814(9), 1210-1218.

Shaked, G.M., Chauv, S., Ubhi, K., Hansen, L.A., Masliah, E., 2009. Interactions between the amyloid precursor protein C-terminal domain and G proteins mediate calcium dysregulation and amyloid beta toxicity in Alzheimer's disease. FEBS J 276(10), 2736-2751.

Shaked, G.M., Kummer, M.P., Lu, D.C., Galvan, V., Bredesen, D.E., Koo, E.H., 2006. Abeta induces cell death by direct interaction with its cognate extracellular domain on APP (APP 597-624). FASEB J 20(8), 1254-1256.

Siskova, Z., Justus, D., Kaneko, H., Friedrichs, D., Henneberg, N., Beutel, T., Pitsch, J., Schoch, S., Becker, A., von der Kammer, H., Remy, S., 2014. Dendritic structural degeneration is functionally linked to cellular hyperexcitability in a mouse model of Alzheimer's disease. Neuron 84(5), 1023-1033.

Sola Vigo, F., Kedikian, G., Heredia, L., Heredia, F., Anel, A.D., Rosa, A.L., Lorenzo, A., 2009. Amyloid-beta precursor protein mediates neuronal toxicity of amyloid beta through Go protein activation. Neurobiol Aging 30(9), 1379-1392.

Van Nostrand, W.E., Melchor, J.P., Keane, D.M., Saporito-Irwin, S.M., Romanov, G., Davis, J., Xu, F., 2002. Localization of a fibrillar amyloid beta-protein binding domain on its precursor. J Biol Chem 277(39), 36392-36398.

Yamatsuji, T., Okamoto, T., Takeda, S., Murayama, Y., Tanaka, N., Nishimoto, I., 1996. Expression of V642 APP mutant causes cellular apoptosis as Alzheimer trait-linked phenotype. EMBO J 15(3), 498-509.

Zhu, X., Rottkamp, C.A., Boux, H., Takeda, A., Perry, G., Smith, M.A., 2000. Activation of p38 kinase links tau phosphorylation, oxidative stress, and cell cycle-related events in Alzheimer disease. J Neuropathol Exp Neurol 59(10), 880-888.

Legends

Figure 1. **Aβ deposition enhances endogenous APP and Goα proteins interaction in dystrophic neurites.** Rat mature hippocampal cultures (10-14 DIV) were treated with vehicle (control) or 20 µM Aβ. After fixation, cultures were labeled with antibodies against APP (clone Y188, followed by Alexa Fluor 568-conjugated anti-rabbit antibody, red) and Goα (clone A2, followed by Alexa Fluor 488-anti mouse antibody, green). Neutravidin-AlexaFluor 350 was used to label biotinylated Aβ (blue). **A.** Images are confocal optical sections taken at 60X magnification. Note that co-localization of APP and Goα is enhanced in dystrophic neurites surrounding large deposits of Aβ (arrows), while in distant neurites the degree of co-localization is similar to control. **B-D.** Interaction of endogenous APP and Goα in primary neurons was determined by FRET using the acceptor photobleaching technique in hippocampal cultures immunolabeled as in **A. B.** Representative images of vehicle- and Aβ-treated cultures showing the fluorescent signal emitted by Goα before and after photobleaching the Alexa Fluor 568-labed APP. Right panels are enlargement of the indicated areas. **C,** Pseudocolor maps showing the mean FRET efficiency (Em) of images shown in **B. D.** Frequency histogram of Em in neuritic segments of cultures treated with vehicle or Aβ. Aβ/np corresponds to Aβ-treated cultures in which primary antibody Y188 was selectively excluded from immunolabeling. Compared to vh and Aβ/np cultures, Aβ treatment significantly increases the frequency of neuritic segments with higher Em while excluding Y188 antibody in Aβ-treated cultures (ct) drastically reduces Em. *$p < 0.001$ by non-parametric X^2 test. Scale bar 10 µm.

Figure 2. APP-overexpression sensitizes hippocampal neurons to Aβ-toxicity through Go protein Gβγ complex signaling. A. Hippocampal cultures were co-transfected with plasmids encoding YFP (40ng/well, pEGFP-N1), human APP (120ng/well, pcDNA3.1) and/or a mutant form of Goα (iPTX-Go, 60ng/well pcDNA3.1) that is insensitive to Pertussis toxin (PTX). Control

cultures were transfected with the corresponding empty vectors (ev). Immediately after transfection cultures were treated with vehicle or 20µM Aβ with or without PTX (0.4 µg/ml) for 8 h. Neuronal viability was assessed by scoring YFP-neurons with healthy morphological appearance and expressed as ratio to the corresponding control condition. Shown are mean ± SEM. a: p=0.0003 vs ev+Aβ and 0.0001 vs APP+ Aβ+PTX; b: p=0.00048 vs APP+ Aβ+PTX and p=0.004 vs ev+Aβ by ANOVA followed by Tukey HSD post hoc test. **B.** Hippocampal cultures were co-transfected plasmids with encoding for YFP, APP, increasing amounts of wild type Goα (wtGoα, 60, 90 and 120 ng/well, pcDNA3.1) or empty vectors. Viability was assessed after 6h treatment with Aβ. Shown are mean ± SEM. c: p=0.00016 vs APP+ev, p=0.039 vs APP+wtGoα90 and p=0.00013 vs APP+wtGoα120 by ANOVA followed by Tukey HSD post hoc test. **C.** Hippocampal cultures were co-transfected with vectors encoding for YFP, APP, β adrenergic receptor kinase C-terminal peptide (βARKct, 120ng/well, pcDNA3.1) or empty vectors. Viability was assessed after 6h of Aβ treatment. Shown are mean ± SEM. d: p=0.0011 vs APP+vh and p=0.034 vs APP+Aβ+ βARKct by ANOVA followed by Tukey HSD post hoc test. **D.** Hippocampal cultures were co-transfected with vectors encoding for YFP, APP or corresponding empty vectors. Viability was assessed after 6h of treatment with Aβ alone or in the presence of gallein (10 µM). Shown are mean ± SEM. e: p=0.013 vs ev+ Aβ and p=0.024 vs APP+Aβ+gallein by ANOVA followed by Tukey HSD post hoc test.

Figure 3. Inhibition of Gβγ complex signaling protects hippocampal neurons from Aβ-induced degeneration and death. Mature hippocampal cultures were treated with vehicle (control) or gallein (10 µM) and 30 min later vehicle or Aβ (20 µM) was added. After 24 and 48 h, cultures were fixed and immuno-labeled with anti-MAP2 antibody. **A.** Representative low-magnification fluorescent images of cultures stained with anti-MAP2 antibody. Experimental conditions are indicated and red arrows point to examples of neurons exhibiting dendritic

dystrophy. **B.** Quantitative assessment of neuronal loss. Data (mean ± SEM) are expressed as neurons per field. a: p=0.00049 vs control and p=0.00176 vs Aβ+gallein 24h; b: p=0.00015 vs control and p=0.0145 vs Aβ+gallein 48h; c: p=0.0017 vs control; ns: not significantly different from control by ANOVA followed by Tukey HSD post-hoc test. **C.** Quantitative assessment of neurons with dystrophic dendrites. Shown are representative images of MAP2-labeled neurons with healthy appearance of dendrites and a dystrophic neuron with collapsed and tortuous dendrites, typical from Aβ-treated culture. Data (mean ± SEM) are expressed as the percentage of dystrophic neurons in each experimental condition. d: p=0.00016 vs control and p=0.00024 vs Aβ+gallein 24h; e: p=0.00152 vs control and p=0.0405 vs Aβ+gallein 48h; ns: not significantly different from control by ANOVA followed by Tukey HSD post-hoc test. **D.** Assessment of total MAP2 fluorescence intensity. Values (mean ± SEM) are expressed in arbitrary units (a.u.). f: p=0.0166 vs control and p=0.0082 vs Aβ+gallein 24h; g: p=0.0043 vs control and p=ns vs Aβ+gallein 48h; ns: not significantly different from control by ANOVA followed by Tukey HSD post-hoc test. **E.** Quantitative estimation of dendritic length. Shown are representative image of MAP2-stained dendrites and the corresponding skeletonization (Image J FIJI software). Mean ± SEM of dendritic length (skeletonize) are expressed in pixels. h: p=0.00018 vs control and p=0.0042 vs Aβ+gallein 24h; i: p=0.00018 vs control and p=0.054 vs Aβ+gallein 48h; j: p=0.0055 vs control; ns: not significantly different from control by ANOVA followed by Tukey HSD post-hoc test. Scale bar 150 µm.

Figure 4. Gallein inhibits Aβ-induced tau pathology revealed by PHF-1 antibody in hippocampal neurons. Mature hippocampal cultures were treated with vehicle (control) or gallein (10 µM) and 30 min later vehicle or Aβ (20 µM) was added. Tau pathology was evaluated 48 h later by fluorescence microscopy after immunolabeling with PHF-1 antibody. **A.** Upper panels show low magnification fluorescent images of hippocampal cultures labeled with PHF-1

antibody. Experimental conditions are indicated. Areas surrounding the red arrows are enlarged in the lower panels. Red arrows points to examples of PHF-1 staining in neuronal somas in the different experimental conditions. Note that gallein prevents Aβ-induced missorting of PHF-1 labeling to the somatodendritic compartment. **B.** Quantitative assessment of somatic PHF-1 immunostaining per field. Data (mean ± SEM) is expressed as number of PHF-1 positive neurons per field. a: p=0.00012 vs control and p=0.00036 vs Aβ+gallein; b: p=0.0037 vs control by ANOVA followed by Tukey HSD post-hoc test. **C.** Assessment of PHF-1 fluorescence intensity in neuronal somas. Data (mean ± SEM) are expressed in arbitrary units. c: p=0.0001 vs control and vs Aβ+gallein; d: p=0.0088 vs control by ANOVA followed by Tukey HSD post-hoc test. **D.** Assessment of total PHF-1 fluorescence intensity per field. Data (mean ± SEM) are expressed in arbitrary units. e: p=0.023 vs control and p=0.0085 vs Aβ+gallein; ns: not significantly different from control by ANOVA followed by Tukey HSD post-hoc test. Scale bar 150 µm.

Figure 5. Gallein protects hippocampal cultures from Aβ-induced synaptic loss. Hippocampal cultures (14 DIV) were treated with vehicle (control), gallein (10 µM) and Aβ (20 µM). After fixation, cultures were immuno-stained with antibodies to PSD95 (red) and synaptophysin (green) and analyzed by high resolution confocal microscopy. Upper left panel shows a representative image of a confocal optical section (60X) of a control hippocampal culture. Monochrome images of individual channels are shown and the indicated squared area is enlarged to allow the appreciation of the complete apposition of synaptophysin and PSD95 clusters, indicative of morphofunctional synaptic contacts. Scale bar 10 µm. Lower left panels show representative images of synaptophysin immunostained cultures under indicated experimental condition. Scale bar 5 µm. Lower right panel shows quantitative assessment of synaptophysin puncta in each experimental condition. Data are mean ± SEM and is expressed as

number of puncta per field. a: p=0.00016 vs control and p=0.0017 vs Aβ+GAL; ns: not significantly different from control by ANOVA followed by Tukey HSD post-hoc test.

Figure 6. Aβ enhanced p38-MAPK activation requires Gβγ complex signaling and is involved in neuronal degeneration. A. p38-MAPK inhibition abrogates APP-dependent toxicity of Aβ. Hippocampal neurons were co-transfected with YFP, APP or empty vector (ev). Then, cultures were treated with vehicle or Aβ (20 µM) with or without the indicated inhibitors. SP600125 (SP, specific inhibitor of c-Jun N-terminal kinase, 1µM), SB (specific inhibitor of p38-MAPK, SB203580 20µM), PD (specific inhibitor of extracellular-regulated kinase, PD98059 50µM) or IPA (specific inhibitor of P21-activated kinase 3, IPA3 5µM). Viability was assessed after 6 h by scoring YFP-neurons with healthy morphological appearance and expressed as ratio to respective vh-treated culture. Shown are mean ± SEM. a: p≤0.019 vs vh; ns: not significantly different from vh by ANOVA followed by Tukey HSD post hoc test. **B.** Effect of Aβ and gallein on p38-MAPK activity.–Mature hippocampal cultures were pre-treated with SB203580 (20 µM) or gallein (10 µM) and 30 min later vehicle or Aβ (20µM) was added. Treatment with H_20_2 (100 µM for 10 min) was used as positive control for p38-MAPK activation. After 3 h of treatment, cultures were lysed and analyzed by western blot with antibodies that recognize p38-MAPK (p38) or p38-MAPK phosphorylated at Thr180/Tyr182 (P-p38). Upper panel shows representative western blot images and lower panel shows densitometry analysis of p38 activation estimated as the ratio of P-p38/p38 in each experimental condition and normalized to control condition. Data are mean ± SEM of five independent experiments. a: p=0.0054 vs control, p=0.023 vs Aβ+SB203580 and p=0.0024 vs Aβ+gallein; b: p=0.01 vs control; ns: not significantly different from control by ANOVA followed by LSD post hoc test. **C-E.** Mature hippocampal cultures were pre-treated with SB203580 (20 µM) and 30 min later vehicle or aggregated Aβ (20 µM) was added. 24 h later, dendritic dystrophy and tau pathology were evaluated by MAP-2 and PHF-1 immunolabeling,

respectively (as shown in Figures 4-5). **C.** Effect of p38MAPK inhibition on Aβ-induced dendritic dystrophy. Quantitative determination of dendritic dystrophy (mean ± SEM) are expressed as the percentage of dystrophic neurons in each experimental condition. a: p=0.00016 vs control and vs Aβ+SB203580; b: p=0.0142 vs Aβ+gallein; b: p=0.00016 vs control; ns: not significantly different from control by ANOVA and Tukey HSD post hoc test. **D-E.** Effect of p38MAPK inhibition on Aβ-induced tau pathology. **D.** Quantitative assessment of somatic PHF-1 immunostaining per field. Data (mean ± SEM) is expressed as number of PHF-1 positive neurons per field. c: p = 0.00016 vs control and vs Aβ+SB203580 by ANOVA followed by Tukey HSD post-hoc test. **E.** Intensity of PHF-1 fluorescence in neuronal somas. Data (mean ± SEM) are expressed in arbitrary units. d: p= 0.00017 vs control and p=0.0069 vs Aβ+SB203580 by ANOVA followed by Tukey HSD post-hoc test.

Figure 7. Inhibition of Gβγ complex signaling by gallein reverses recognition memory impairment in 3xTg-AD mice. **A**. Scheme of experimental design. Wild-type (WT) and 3xTg-AD (Tg) mice were daily handled, exposed to context for habituation. 90 min before de training session mice were bilaterally administered with vehicle (vh) or gallein (50 ng/hippocampus) into de dorsal hippocampus (dHIP), and were tested 24 h later. **B**. Discrimination index (D.I.) in the new object recognition test are shown as mean ± SEM. ***p=0.0046; **p=0.0105 by ANOVA and Tukey HSD post-hoc test. **C**. Mouse atlas sections (Franklin & Paxinos, 1997) corresponding to the injection site. Distance from Bregma is shown and black squares indicate tip of infusion syringe.

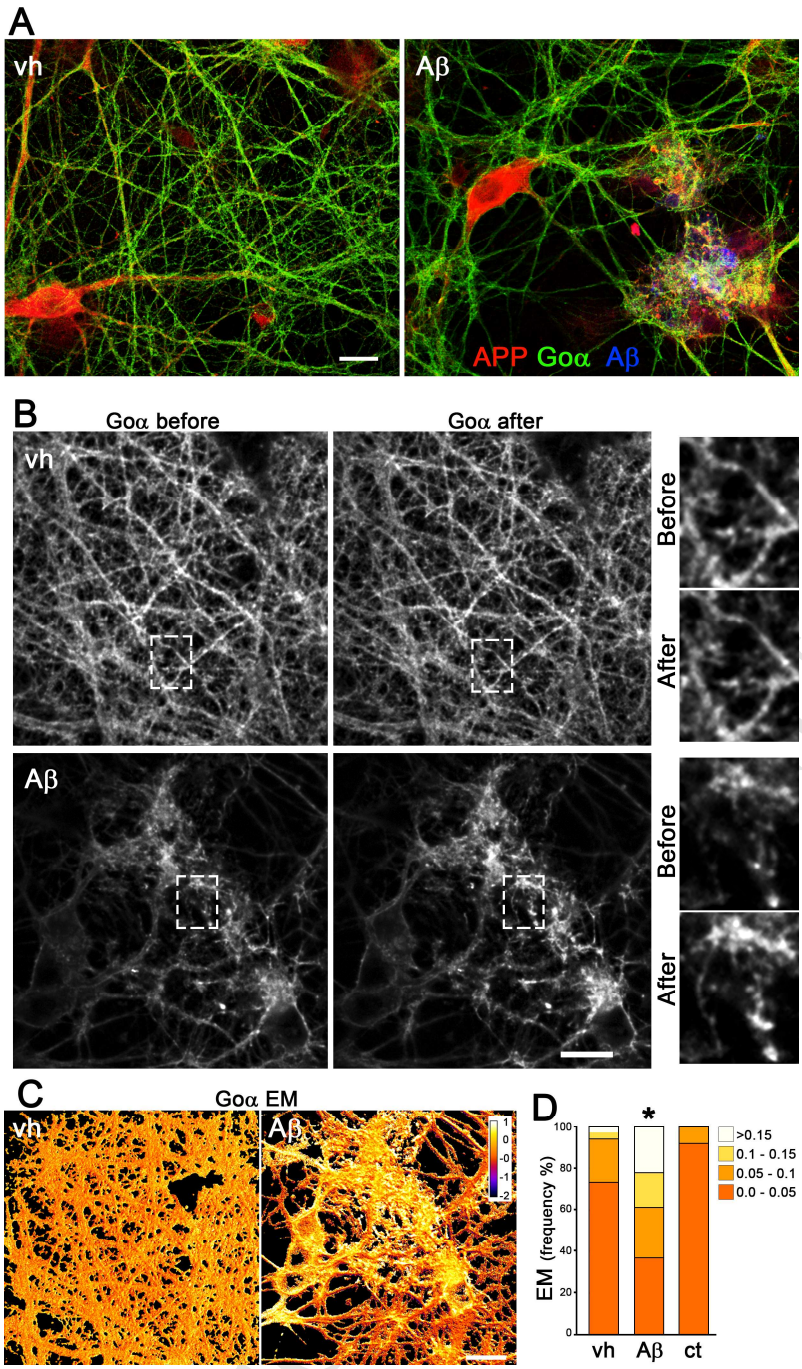
A
vh
Aβ
APP Goα Aβ
B
Goα before
Goα after
vh
Before
After
Aβ
Before
After
C
Goα EM
vh
Aβ
1
0
-0
-1
-2
D
*
EM (frequency %)
100
80
60
40
20
0
vh
Aβ
ct
>0.15
0.1 - 0.15
0.05 - 0.1
0.0 - 0.05

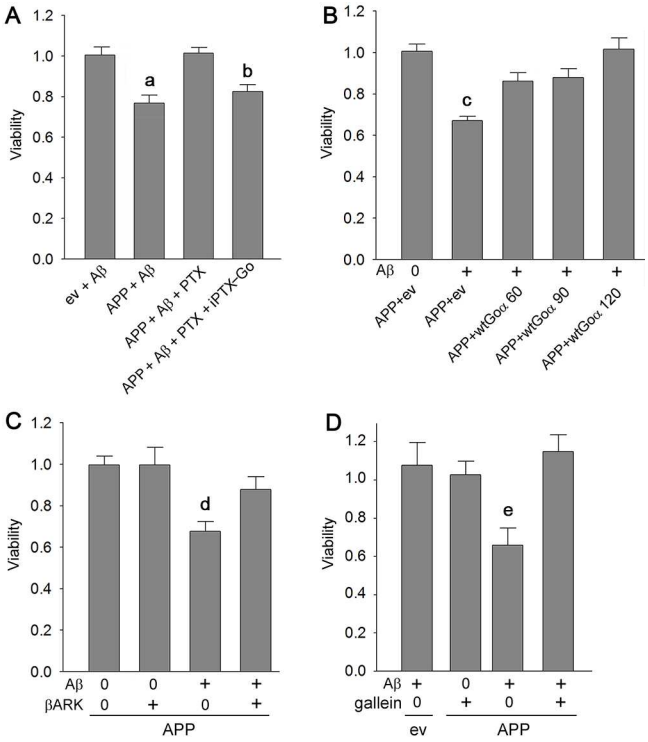

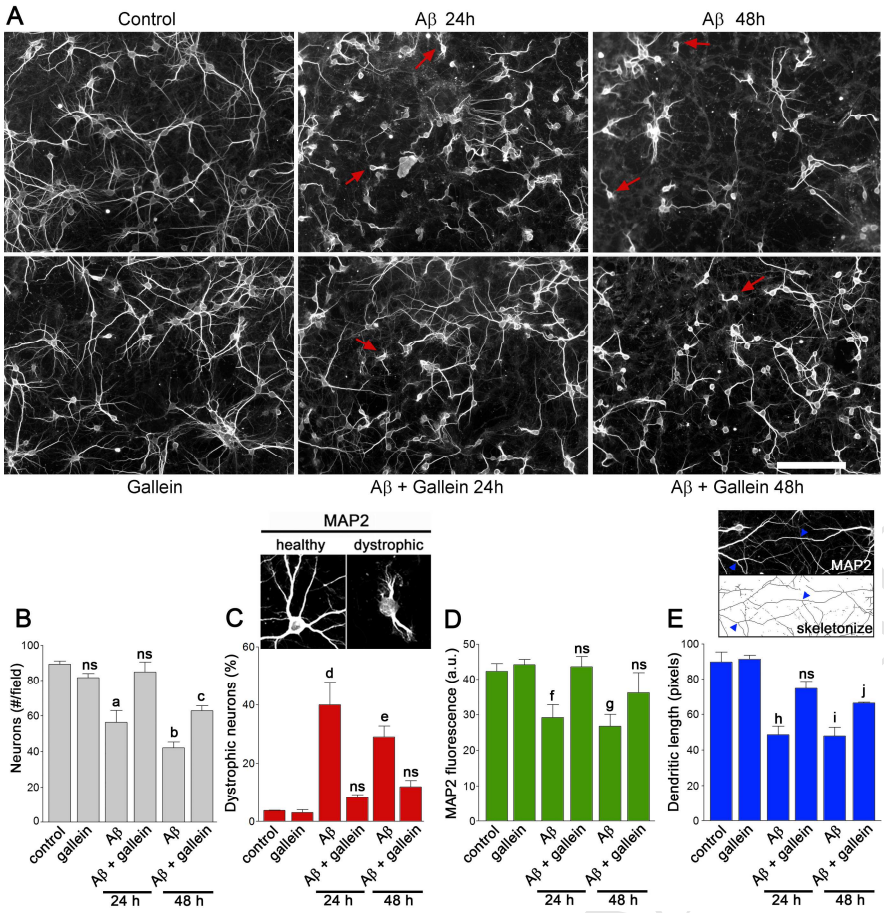

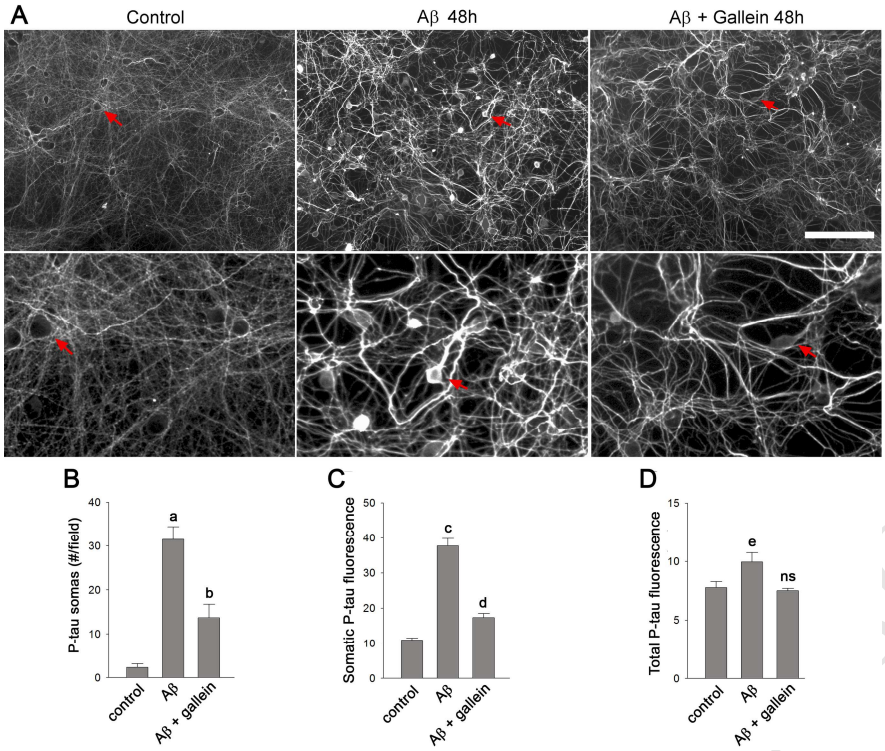

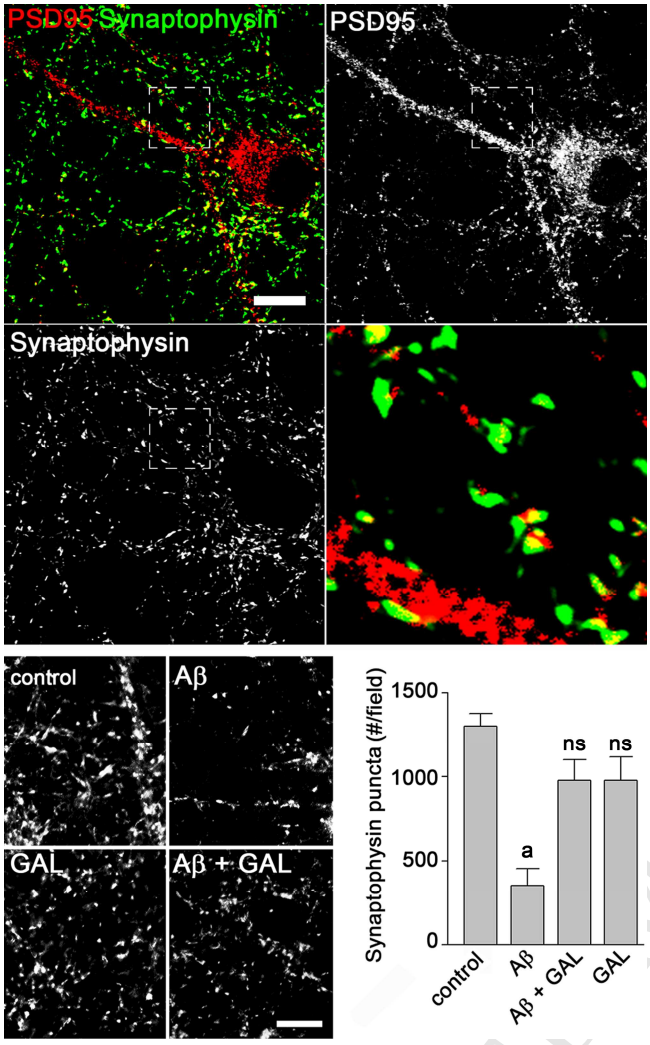

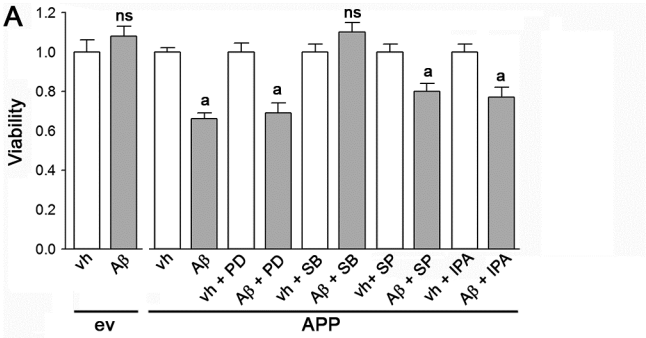
A
Viability
1.2
1.0
0.8
0.6
0.4
0.2
0.0
ns
a
a
ns
a
a
vh
Aβ
vh
Aβ
vh + PD
Aβ + PD
vh + SB
Aβ + SB
vh+ SP
Aβ + SP
vh + IPA
Aβ + IPA
ev
APP

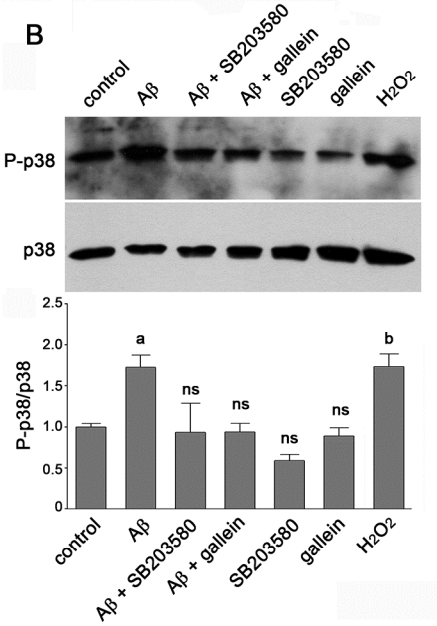
B
control
Aβ
Aβ + SB203580
Aβ + gallein
SB203580
gallein
H2O2
P-p38
p38
P-p38/p38
2.5
2.0
1.5
1.0
0.5
0
a
ns
ns
ns
ns
b
control
Aβ
Aβ + SB203580
Aβ + gallein
SB203580
gallein
H2O2

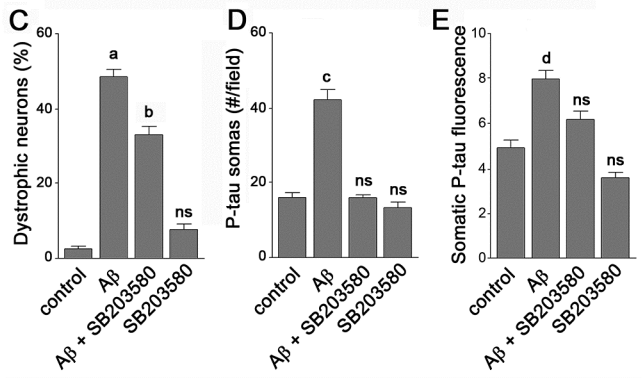
C
Dystrophic neurons (%)
60
40
20
0
a
b
ns
control
Aβ
Aβ + SB203580
SB203580
D
P-tau somas (#/field)
60
40
20
0
c
ns
ns
control
Aβ
Aβ + SB203580
SB203580
E
Somatic P-tau fluorescence
10
8
6
4
2
0
d
ns
ns
control
Aβ
Aβ + SB203580
SB203580